Theor Chem Acc (2009) 124:187–195
DOI 10.1007/s00214-009-0599-8

REGULAR ARTICLE

A theoretical study of diborenes HLB=BLH for L=CO, NH_3, OH_2, PH_3, SH_2, ClH: structures, energies, and spin–spin coupling constants

Ibon Alkorta · Janet E. Del Bene · José Elguero · Otilia Mó · Manuel Yáñez

Received: 14 May 2009 / Accepted: 10 June 2009 / Published online: 27 June 2009

Abstract Ab initio calculations were carried out to investigate the structures, binding energies, bonding, and NMR spin–spin coupling constants of complexes HLB=BLH, for L=CO, NH_3, OH_2, PH_3, SH_2, and ClH. Both B–B and B–H bonds lengthen on complex formation relative to singlet HBBH, and except for L=CO, the B–B bonds are double bonds. The order of stability of the *trans* isomers correlates with the ordering of ligands in the spectrochemical series of ligand field theory. The *trans* isomer is always more stable than the corresponding *cis*. Inverse correlations are found between ^1J(B–B) and ^1J(B–H) and the corresponding B–B and B–H distances. For the *trans* isomers, ^1J(B–B) appears to be related to the ordering of ligands in the spectrochemical series, while ^1J(B–H) is related to the protonation energy of the ligand L.

Keywords Diborenes · Spectrochemical series · AIM · ELF · NMR coupling constants

Electronic supplementary material The online version of this article (doi:10.1007/s00214-009-0599-8) contains supplementary material, which is available to authorized users.

I. Alkorta (✉) · J. Elguero
Instituto de Química Médica (CSIC), Juan de la Cierva, 3, 28006 Madrid, Spain
e-mail: ibon@iqm.csic.es

J. E. Del Bene
Department of Chemistry, Youngstown State University, Youngstown, OH 44555, USA

O. Mó · M. Yáñez
Departamento de Química, C-9, Universidad Autónoma de Madrid, Cantoblanco, 28049 Madrid, Spain

1 Introduction

Boron is an element that presents a variety of chemical bonding motifs, starting with its allotropic forms and continuing in the boranes, metalloboranes, carboranes (among them the strongest superacids), metallocarboranes, boron halides, borates, and finally, boron–nitrogen compounds [1–3]. In recent papers, we have focused on various series of related molecules with B–N bonds, and have investigated their structural, energetic, and NMR spectroscopic properties [4–6]. These studies also included a recently synthesized organoboryl compound [7] in which boron acts as a nucleophile [8]. In the present study, we turn our attention to systems with B–B multiple bonds, a few of which have been described in the literature [9–17] Among them are those with a B–B triple bond L–B≡B–L (**I**) and a B–B double bond HLB=BLH (**II**) stabilized by two carbenes, as illustrated in Fig. 1. In the present study, we investigate model systems for **II**, represented as HLB=BLH, for L a set of neutral Lewis bases (ligands) CO, NH_3, OH_2, PH_3, SH_2, and ClH, with the ligands in *trans* and *cis* positions (**1**-*E* and **1**-*Z*, respectively), as shown in Fig. 2.

In the *E* and *Z* isomers, the two ligands (L_5 and L_6) are identical, but are numbered to show that H_3 and L_5 are always bonded to B_1, and H_4 and L_6 to B_2. X_5 and X_6 are the electron-donor atoms in L_5 and L_6, respectively, which form the bonds to B_1 and B_2. In this study, we describe the geometric and electronic structures and bonding properties of the *trans* and *cis* isomers, binding energies of the complexes, and NMR spin–spin coupling constants.

2 Methods

DFT calculations employing the B3LYP functional [18, 19] and the 6-311++G(d,p) basis set [20] were carried out

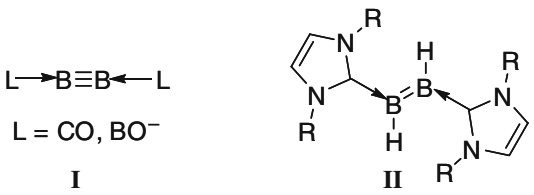

Fig. 1 Structures of compounds **I** and **II**

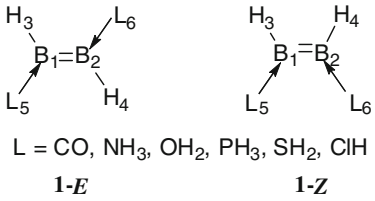

Fig. 2 Structures of compounds **1-*E*** and **1-*Z***

to optimize the structures of all complexes in both singlet and triplet states, using the Gaussian-03 package [21]. Frequency calculations were performed to confirm that the optimized structures correspond to minima on the potential surfaces. Stability checks were made to identify and eliminate systems which have RHF/UHF instabilities. The structures of the singlet states were also optimized at second-order Møller–Plesset perturbation theory (MP2) [22–25] with the 6-31+G(d,p) basis set [26–29]. Frequency calculations were performed at this level to insure that these structures were also minimum-energy structures.

The electron densities of these systems have been analyzed using the Atoms in Molecules method [30] with the AIMPAC program [31]. Within this methodology, the bonds are characterized by a (3, −1) stationary point that is designated the bond critical point (bcp). Properties of the bcp including the electron density (ρ), ellipticity (ε), and energy density (H) allow for classification of the bcp. The total energy density, H, has become the preferred alternative to the Laplacian of the electron density ($\nabla^2\rho$), since it overcomes some of the limitations of the latter [32].

In addition, the electron localization functions (ELFs) [33, 34] have been evaluated for these complexes using the ToPMoD package [35]. This function measures the probability that a pair of electrons will be found in a given region of space and has bounds between 0 and 1. ELF isosurfaces around 0.75 provide clear pictures of the regions of electron localization or attraction basins, which may be related to key bonding concepts, such as core, valence, and lone-pair regions. Their populations have been related to bond order.

The natural bond orbital (NBO) [36] approach was employed to analyze bonding in terms of localized hybrids and lone pairs, and to evaluate the nature and weight of resonance structures that may contribute to the stability of a given system. These NBO calculations were carried out allowing for the detection of three-center bonding, which is rather common in boron compounds. However, no three-center bonds were detected in any of these complexes. The interactions between occupied and unoccupied MOs associated with electron donation and back donation arising between the ligands and B_2H_2 were investigated through a second-order perturbation analysis of the Fock matrix. In addition, the Wiberg natural bond orders were computed.

Spin–spin coupling constants were computed for these complexes at the MP2/6-31+G(d,p) geometries using the equation-of-motion coupled-cluster singles and doubles method (EOM-CCSD) in the configuration interaction (CI)-like approximation [37–40] with all electrons correlated. The Ahlrichs qzp basis set [41] was used on ^{13}C, ^{15}N, ^{17}O, and ^{19}F atoms, and the qz2p basis set was used for ^{31}P, ^{33}S, ^{35}Cl, and the ^{1}H atoms bonded to B. The recently constructed hybrid basis set was used for ^{11}B [4]. This basis set has the same number of contracted functions (6s, 4p, and 1d) as the Ahlrichs qzp basis used for C, N, O, and F, and was used previously in studies of B–N, B–H, and B–Li coupling constants [4, 6, 8]. The Dunning cc-pVDZ basis set [42, 43] was placed on H atoms of the ligands. In the nonrelativistic approximation, the nuclear spin–spin coupling constant is composed of four terms: the paramagnetic spin orbit (PSO), diamagnetic spin orbit (DSO), Fermi contact (FC), and spin dipole (SD) [44]. All terms were computed for all complexes. The EOM-CCSD calculations were carried out using ACES II [45] on the Itanium cluster at the Ohio Supercomputer Center.

3 Results and discussion

3.1 Geometries

The geometry and a selection of the structural parameters describing the optimized geometries of the HLB=BLH complexes are shown in Fig. 3 and Table 1. No stable structures were found for *trans* or *cis* isomers with FH as the Lewis base, or for the *cis* isomers which have OH_2 or ClH bonded to the two B atoms. These molecules are relatively poor electron donors. In addition, complexes with N_2, BF, CH_2, and CF_2 have not been included because they present RHF/UHF instabilities. For the OH_2, SH_2, and ClH complexes in the *E* configuration and SH_2 in the *Z* configuration, several minima were located, some of which have similar geometrical and energetic characteristics. However, only the most stable *E* and *Z* configurations have been considered in this study.

The optimized B–B distances in the HLB=BLH systems are similar to the distance reported for compound **II** [1.561 (18) Å] [10], which suggests that these molecules are

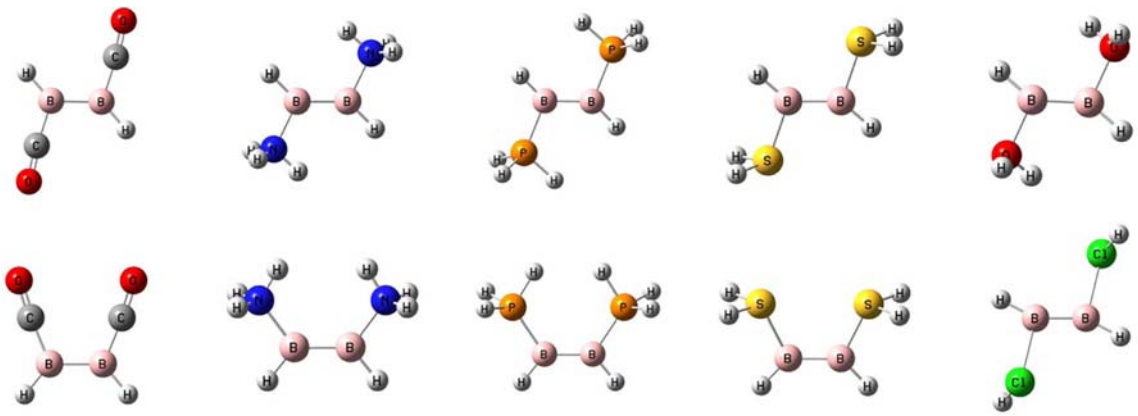

Fig. 3 Optimized MP2/6-31+G(d,p) *cis* and *trans* complexes HLB=BLH

Table 1 Distances (R, Å) and angles (<, °) for optimized MP2/6-31+G(d,p) complexes HLB=BLH[a]

L	Sym.	R (B–B)	R (B_1–H_3)	R (B_1–X_5)	<H_3–B_1–B_2	<X_5–B_1–B_2
CO (**1-*E***)	C_{2h}	1.605	1.184	1.490	132.5	106.7
CO (**1-*Z***)	C_{2v}	1.611	1.185	1.492	129.3	112.3
NH_3 (**1-*E***)	C_{2h}	1.558	1.204	1.625	134.9	115.2
NH_3 (**1-*Z***)	C_{2v}	1.561	1.199	1.645	128.3	126.2
OH_2 (**1-*E***)	C_2	1.552	1.191	1.678	141.5	112.0
PH_3 (**1-*E***)	C_{2h}	1.571	1.194	1.890	134.6	109.7
PH_3 (**1-*Z***)	C_{2v}	1.576	1.196	1.887	127.8	122.9
SH_2 (**1-*E***)	C_{2h}	1.559	1.191	1.910	137.7	108.0
SH_2 (**1-*Z***)	C_{2v}	1.568	1.191	1.904	132.3	115.7
ClH (**1-*E***)	C_i	1.538	1.180	2.106	150.9	104.7

[a] Singlet HBBH: R(B–B) = 1.520 Å; R(B–H) = 1.170 Å; <H_3–B_1–B_2 = 180.0°

reasonable models for a B=B double bond and can be used to analyze bonding and other properties in compounds such as **II**. A compound with a B–B single bond, which is a derivative of **II,** has a much longer B–B distance of 1.828 (4) Å [10].

Not surprisingly, the B1-X5 distances vary significantly with the position in the periodic table of atom (X) in the Lewis base (L), which binds to B. Those molecule with X a second-period atom, have distances between 1.490 and 1.678 Å; those from the third-period have distances between 1.887 and 2.106 Å. If the structures of the ***E*** isomers with the second- and the third-period ligands are compared separately, a correlation is found between the B–X and the B–B distances. That is, the shorter the B–X distance, the longer the B–B distance, which suggests that an increase in the B–X interaction weakens the B–B bond. Similarly, for the *Z* isomers, the B–B bond is longer and the B–X bond shorter when L is PH_3 compared to SH_2, and when L is CO compared to NH_3. The bonding peculiarities which give rise to these differences will be discussed below. The B–B bond is always longer in the *Z* isomer compared to the corresponding *E* isomer. Table 1 also shows a significant lengthening of the BH bonds in the complexes compared to singlet HBBH. It is also interesting to note that within each subset of isomers, larger values of the H_3–B_1–B_2 angle correspond to longer B–X distances, which suggests that these molecules are approaching a nearly linear HBBH and two isolated L molecules.

3.2 Energetics

Although it is well established that HBBH has a triplet ground state ($^3\Sigma_g^-$) [46, 47], the singlet electronic configuration of the complexes HLB=BLH is more stable than the triplet, that is, all complexes are ground-state singlets. The energy difference between the singlet ground state and the lowest triplet state of these complexes varies from 17 to 36 kcal mol^{-1}. As evident from Table 2, the *E* configuration (*trans*) is always more stable than *Z* (*cis*), with the energy difference varying from 1.64 kcal mol^{-1} when L is CO, to 12.18 kcal mol^{-1} when L is NH_3. Several factors are responsible for such differences. A perusal of the NBO second-order interaction energies shows that the population of the π_{BB} bonding orbital is slightly larger in the *E* than in the *Z* isomer. This suggests that the electron-donating ability of the ligands in enhanced in the *E* isomer, and is reflected in a slightly greater B=B bond order in this

Table 2 Symmetries, total energies (a.u.), relative energies of *trans* and *cis* isomers (E_{rel}, kcal mol^{-1}), and binding energies (ΔE, kcal mol^{-1}) of complexes HLB=BLH at MP2/6-31+G(d,p)

L	Sym	Total energy	E_{rel}	ΔE^a
CO (**1-*E***)	C_{2h}	−276.737068	0.00	−86.69
CO (**1-*Z***)	C_{2v}	−276.734449	1.64	−85.05
NH_3 (**1-*E***)	C_{2h}	−163.4296404	0.00	−65.82
NH_3 (**1-*Z***)	C_{2v}	−163.410225	12.18	−53.63
OH_2 (**1-*E***)	C_2	−203.049908	0.00	−27.00
PH_3 (**1-*E***)	C_{2h}	−735.8142017	0.00	−70.94
PH_3 (**1-*Z***)	C_{2v}	−735.801473	7.99	−62.96
SH_2 (**1-*E***)	C_{2h}	−848.231271	0.00	−41.85
SH_2 (**1-*Z***)	C_{2v}	−848.2249686	3.95	−37.89
ClH (**1-*E***)	C_i	−970.958501	0.00	−1.64

[a] ΔE = E(HLB=BLH) − E(HBBH, singlet) − 2E(L)

isomer. Moreover, the electron density at the B=B bcp is slightly greater in the *E* than in the *Z* isomer, and the weight of the resonance structure bearing a B=B double bond is also greater. These differences also increase in going from the second-period ligand NH_3 to the corresponding third-period ligand PH_3, the only case for which such a comparison can be made.

A second important contributor to the lower stability of the *Z* isomers is the increased steric hindrance between the substituents in this conformation, as illustrated in Fig. 4 for L=NH_3 and PH_3. These renderings show the close proximity of the ELF basins associated with NH and PH bonds in the *Z* configuration. The much larger positive charge of the hydrogen atoms when the ligand is NH_3 leads to much stronger ligand–ligand repulsion and results in significant destabilization.

Interaction energies, evaluated relative to HBBH in its lowest singlet state, are also reported in Table 2. Since the energy difference between the ground-state triplet and the first excited singlet state of HBBH is 18 kcal mol^{-1}, all of the complexes are also stable relative to the triplet ground state of HBBH, except for H(HCl)B=B(ClH)H, which is bound by only 1.6 kcal mol^{-1} relative to singlet HBBH. In contrast, the complexes of HBBH with CO have interaction energies, which approach those of covalent bonds. The reasons for such differences will become apparent when the details of the bonding in these systems are discussed below. The order of stabilization energies for these complexes (CO > PH_3 > NH_3 > SH_2 > OH_2 > ClH) is consistent with the ordering of these molecules as ligands in the spectrochemical series of crystal field theory (CO > PR_3 > NH_3 > SR_2 > OH_2), based on their binding strength to metal ions [1a]. This is not unexpected since in both situations, these molecules act as electron-pair donors to an electron-deficient site.

3.3 Bonding analyses

The electron densities, ρ, computed at the bond critical points (bcp) of the *cis* and *trans* isomers of HLB=BLH are reported in Table 3. The values of the B–B and B–H electron densities at the bcps and the negative sign of the total energy density (*H*) indicate shared shell interactions similar to those found for covalent bonds. In contrast, the B–X bcps can be considered as borderline cases, since H is negative while its Laplacian is positive. This combination is usually found for very polar covalent bonds and for strong intermolecular hydrogen bonds [48].

Several reports have shown an exponential relationship between the value of the electron density at the bcp and the interatomic distance [49–51]. In those cases, the interatomic distances were relatively long. In the HLB=BLH complexes, the electron densities and Laplacians at the bcps increase in absolute value as the B–B and B–H distances decrease, as expected. However, both linear and exponential relationships between these variables yield similar correlation coefficients (R^2 always larger than 0.95 for ρ and 0.9 for $\nabla^2\rho$), most probably due to the small range of B–B and B–H distances.

An interesting characteristic of the electron distributions in the HLB=BLH complexes except for L=CO is the high value of the ellipticity (ε) at the B–B bcp, as shown in Table 3. At the same computational level, ε for the C–C bond of ethylene is 0.33. Thus, the value of this parameter is a clear indication of the double bond character of the B=B bond. In addition, the ELF plots of Fig. 5 show disynaptic basins, one on each side of the σ_h symmetry plane, similar to those observed for ethylene. The integrated electron densities within the basins range from 2.63e in the complex with CO to 3.83e in that with OH_2, bracketing the value of 3.37e for ethylene. These results are also a clear indication of the presence of a B=B double bond, with the degree of double bond character varying along the series. This is also illustrated by the Wiberg B–B bond orders, which are reported in Table 4.

As noted above, if the second- and third-row ligands are considered separately, an overall correlation exists between the electron-donating ability of L as measured by its position in the spectrochemical series, and the B–X and B–B bond lengths. In these complexes, as the length of the B–X bond decreases, that of the B–B bond increases. Does a similar relationship extend to the bonding in these molecules, that is, does an increasing B–X bond order correlate with a decreasing B–B bond order? Table 4 reports the Wiberg bond orders for the *E* isomers of HLB=BLH. For complexes with third-period molecules as ligands, the B–B bond order increases as the B–X bond order decreases, and the B–B bond order in the complex with ClH approaches that of HBBH. This is not surprising, given that this

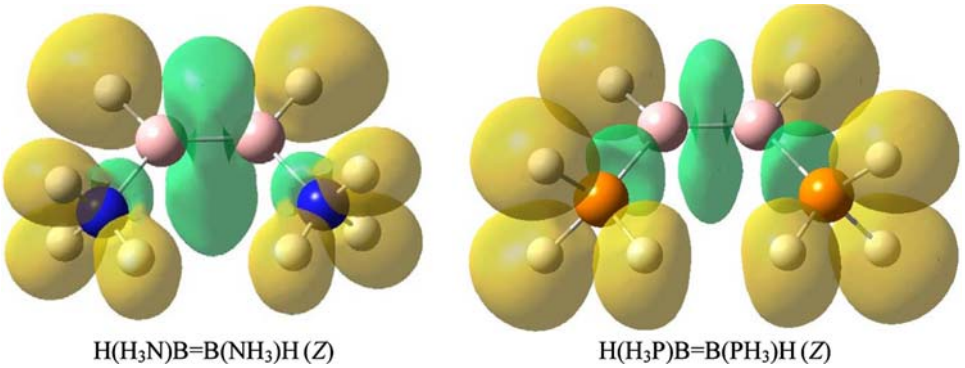

Fig. 4 ELF basins at 0.8 level illustrating steric hindrance in the *Z* isomers of $H(H_3N)B{=}B(NH_3)H$ and $H(H_3P)B{=}B(PH_3)H$

Table 3 The electron density (ρ, a.u.), total energy density (H, a.u.), and ellipticity (ε) at bond critical points for complexes HLB=BLH calculated at B3LYP/6-311++ G(d,p)

L	B=B			B–H		B–X	
	ρ	H	ε	ρ	H	ρ	H
CO (**1-*E***)	0.167	−0.133	0.17	0.176	−0.183	0.162	−0.133
CO (**1-*Z***)	0.168	−0.133	0.16	0.175	−0.182	0.162	−0.134
NH_3 (**1-*E***)	0.187	−0.157	0.46	0.165	−0.164	0.108	−0.065
NH_3 (**1-*Z***)	0.182	−0.151	0.48	0.168	−0.171	0.102	−0.060
OH_2 (**1-*E***)	0.192	−0.165	0.56	0.176	−0.182	0.072	−0.034
PH_3 (**1-*E***)	0.178	−0.145	0.25	0.169	−0.172	0.115	−0.096
PH_3 (**1-*Z***)	0.174	−0.140	0.24	0.169	−0.172	0.116	−0.097
SH_2 (**1-*E***)	0.186	−0.156	0.33	0.175	−0.180	0.096	−0.071
SH_2 (**1-*Z***)	0.182	−0.149	0.31	0.176	−0.182	0.098	−0.073
ClH (**1-*E***)	0.197	−0.175	0.62	0.187	−0.201	0.038	−0.009

complex is very weakly bound. However, a correlation between B–B and B–X bond orders does not appear to exist for complexes in which a second-period atom is the electron donor. The complex with L=CO is unique and will be discussed in detail. For the complexes with $L{=}NH_3$ and H_2O, the B–X bond order decreases with $NH_3 > H_2O$ as anticipated, but the B–B bond orders are similar to that of HBBH, and therefore appear to be too high. Closer examination of Table 4 suggests that the B–B bond order may not be very sensitive to the nature of the ligand, except for complexes with $L{=}PH_3$ and H_2S. What factors are responsible for these observations?

Complex formation formally changes the hybridization of B from *sp* to sp^2, thereby decreasing the intrinsic

Table 4 Wiberg bond orders for the *E* isomers of HLB=BLH[a]

Bond	CO[b]	NH_3	H_2O	PH_3	SH_2	ClH
B–X	1.20	0.63	0.45	1.02	0.89	0.38
B–B	1.31	1.91	1.98	1.70	1.72	1.97

[a] The Wiberg B–B bond order for singlet HBBH is 1.977

[b] The C–O bond order in the complex is 2.10

electronegativity of B and increasing the length of both B–B and B–H bonds. Moreover, as the electron-donating ability of L increases, the degree of charge transfer to B increases, thereby increasing the net negative charge at B, as evident from Table 5. The order of decreasing negative charge on B follows the order of the spectrochemical series, with a reversal of NH_3 and SH_2. The accumulation of negative charge on the two B atoms results in an increased electrostatic repulsion between them and a lengthening of the B–B bond. If a direct correlation between B–B bond length and B–B bond order exists, then both of these factors should lead to a decrease of the B–B bond order in all complexes, but this is not supported by the data of Table 4.

The B–B bond may also be influenced by three different orbital interactions, which can be described by NBO analyses. The first of these involves charge transfer from the σ_{BH} bonding orbital, which gains electron density on complexation, to the σ^*_{BB} antibonding orbital. The interaction energy is reported as ΔE_1 in Table 5. The trend in ΔE_1 parallels the spectrochemical series of the ligands, again with a reversal of H_2S and NH_3. The largest effects are found for the complexes in which the charge on B is greatest, namely, complexes with $L{=}PH_3$ and H_2S.

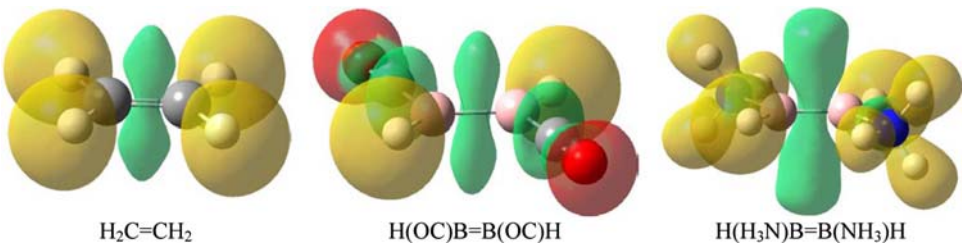

Fig. 5 ELF isosurfaces at values of 0.75 for $H_2C{=}CH_2$, $H(OC)B{=}B(CO)H$, and $H(H_3N)B{=}B(NH_3)H$ computed at B3LYP/6-311++G(d,p)

Table 5 Net natural atomic charge at the boron atom [q(B)] and orbital interaction energies [ΔE_1, ΔE_2, and ΔE_3, (kcal mol^{-1})] for the *trans* isomers of HLB=BLH[a]

L	q(B)[b]	ΔE_1	ΔE_2	ΔE_3
CO (**1-*E***)	–0.304	12.0[c]	–	–
NH_3 (**1-*E***)	–0.258	2.2	2.1	1.1
OH_2 (**1-*E***)	–0.184	0.6	0.6	0.6
PH_3 (**1-*E***)	–0.542	3.7	6.9	0.8
SH_2 (**1-*E***)	–0.371	3.1	7.6	1.0
ClH (**1-*E***)	–0.137	<0.5[d]	1.5	<0.5[d]

[a] ΔE_1, ΔE_2, and ΔE_3 are orbital interaction energies, which are defined in the text

[b] The charge on B for singlet HBBH is +0.135

[c] This interaction energy corresponds to back donation from the π_{BB} bonding orbital into the π^*_{CO} antibonding orbital

[d] Values less than 0.5 kcal mol^{-1} are not reported

For these two complexes, ΔE_1 values are 3.7 and 3.1 kcal mol^{-1}, respectively. In contrast, ΔE_1 for NH_3 and H_2O are 2.2 and 0.6 kcal mol^{-1}, respectively.

The next two orbital interactions are of the hyperconjugative type, the first and stronger one involving the π_{BB} bonding orbital and the pseudo-π^*_{XH} antibonding orbital formed from the σ^*_{XH} antibonding orbitals of the X–H bonds, which lie above and below the plane defined by HBBH. This interaction removes electron density from the π_{BB} bonding orbital. As evident from Table 5, this interaction is significantly stronger for the complexes formed from PH_3 and H_2S for which ΔE_2 is 6.9 and 7.6 kcal mol^{-1}, respectively, compared to the remaining complexes which have ΔE_2 values between 0.6 and 2.1 kcal mol^{-1}. The second hyperconjugative-type interaction involves another pseudo-π orbital formed from the σ_{XH} bonding orbitals of the ligands interacting with the π^*_{BB} antibonding orbital. This interaction populates the B–B antibonding orbital, but is a significantly weaker interaction with ΔE_3 values of 1.1 kcal mol^{-1} or less. Thus, while all of the factors considered above are consistent with an increase in the B–B bond distance, the B–B bond orders of the *trans* isomers are significantly reduced only when PH_3 and H_2S are the ligands. This suggests that the reduction in the computed B–B bond orders in these two complexes should be attributed primarily to the strong hyperconjugative π_{BB}–π^*_{XH} interaction, reinforced by the σ_{BH}–σ^*_{BB} interaction.

The *E* isomer of H(OC)B=B(CO)H shows a different pattern with a large interaction energy and B–X bond order, but low B=B bond order. This is a result of the ability of CO to act as a good σ-electron donor through C and at the same time a good π-electron acceptor, as is well known in coordination chemistry. An NBO analysis shows the existence of a σ_{BC} covalent bond, as well as back donation from the π_{BB} bonding orbital into the π^*_{CO} antibonding orbital.

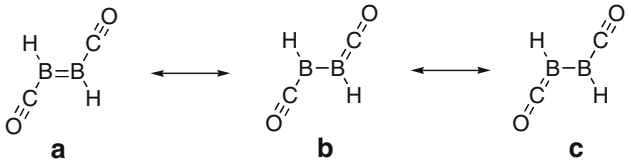

Fig. 6 Natural resonance theory (NRT) analysis

This back donation is responsible for an increase in the C–B bond order and depopulation of the π_{BB} bond, and is reflected not only in a low population at the corresponding basin as noted above, but also in a significant decrease of the B=B bond order. Electron transfer to the π^*_{CO} antibonding orbital also leads to a significant decrease of the CO bond order, which becomes lower than that of isolated CO (2.27). Moreover, a natural resonance theory (NRT) analysis indicates that although the resonance structure ***a*** of Fig. 6 has a weight of 33%, there are two other important equivalent contributors, ***b*** and ***c***, with weights of 20% each, which increase the bond order of the B–C bond while reducing that of the C–O bond. Only structures like ***a*** contribute to the B–X bonds in the other complexes, and these remain single bonds.

3.4 Coupling constants

The calculated coupling constants (J) for the *trans* and *cis* isomers of the HLB=BLH complexes are reported in Table 6. The components of these coupling constants can be found in the supporting information. From these data, it is apparent that all one-bond B–B and B–H coupling constants are dominated by the Fermi-contact term. Since the magnetogyric ratios of ^{11}B and ^{1}H are positive and all one-bond B–B and B–H coupling constants are large and positive, the reduced coupling constants ^1K(B–B) and ^1K(B–H) are positive and consistent with the Dirac Vector Model [52]. The B–B coupling constant ^1J(B–B) is greater in the *cis* isomer except when L=SH_2. The one-bond coupling constants ^1J(B–H) are similar in magnitude in corresponding *trans* and *cis* isomers, except when L=NH_3, in which case ^1J(B–H) is 9 Hz greater in the *cis* isomer. ^1J(B–H) is approximately an order of magnitude greater than ^2J(B–H), which may be either positive or negative.

In order to compare the signs of B–X coupling constants in different complexes, it is necessary to use reduced coupling constants since the magnetogyric ratios of ^{15}N and ^{17}O are negative while those of ^{13}C, ^{31}P, ^{33}S, and ^{35}Cl are positive. An examination of Table 6 indicates that the reduced one-bond coupling constants ^1K(B–X) may be positive or negative, while the reduced two-bond coupling constants ^2K(B-X) are positive, except for ^2K(B–C) for the *trans* isomer of H(OC)B=B(CO)H. ^1J(B–X) values are also similar in corresponding *trans* and *cis* isomers except when

Table 6 One-bond B–B, B–H, and B–X, and two-bond B–H and B–X spin–spin coupling constants (J, Hz) for *trans* and *cis* isomers of HLB=BLH

L	Sym	^1J(B1–B2)	^1J(B1–H3)	^1J(B1–X5)	^2J(B1–H4)	^2J(B1–X6)
CO (**1-*E***)	C_{2h}	61.1	145.1	61.3	–7.8	–3.7
NH_3 (**1-*E***)	C_{2h}	126.4	107.5	–1.0	9.0	–8.4
OH_2 (**1-*E***)	C_2	148.8	129.1	13.8	14.7	–8.7
PH_3 (**1-*E***)	C_{2h}	98.2	128.7	32.8	–0.7	38.1
SH_2 (**1-*E***)	C_{2h}	125.0	135.7	–11.0	5.8	25.0
ClH (**1-*E***)	C_i	178.3	163.7	–15.3	17.9	20.1
CO (**1-*Z***)	C_{2v}	71.2	147.2	62.4	–10.8	0.1
NH_3 (**1-*Z***)	C_{2v}	130.1	116.4	0.8	12.3	–2.3
PH_3 (**1-*Z***)	C_{2v}	106.5	124.8	47.8	–1.6	12.8
SH_2 (**1-*Z***)	C_{2v}	120.8	133.5	–8.9	12.1	10.4

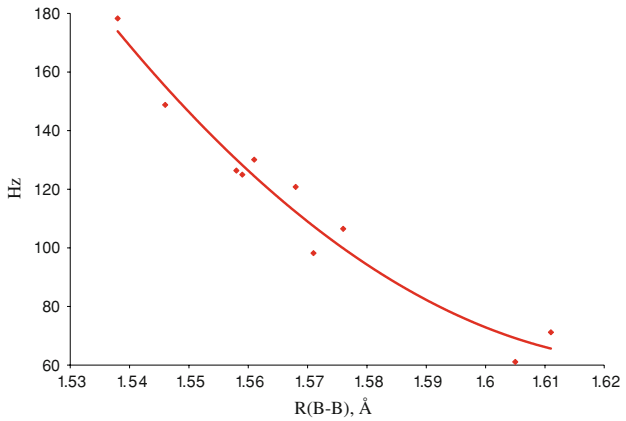

Fig. 7 ^1J(B–B) versus the B–B distance for HLB=BLH

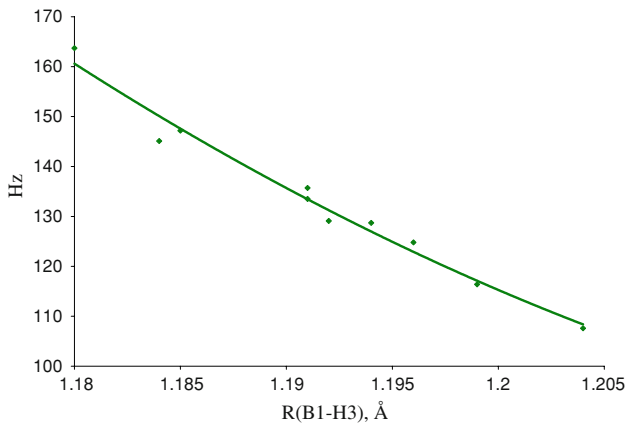

Fig. 8 ^1J(B1–H3) versus the B1–H3 distance for HLB=BLH

L=PH_3, in which case ^1J(B–P) is 15 Hz larger in the *cis* isomer.

Figure 7 shows a plot of ^1J(B–B) versus the B–B distance, and Fig. 8 shows a similar plot of ^1J(B1–H3) versus the B1–H3 distance. The trend lines are second-order curves with correlation coefficients of 0.962 and 0.978, respectively. These curves indicate that as the B–B and B–H distances decrease, the B–B and B–H coupling constants tend to increase in this closely related series of complexes. However, it should be noted that although the *E* isomer has the shorter B–B distance, ^1J(B–B) for the *Z* isomer is greater than ^1J(B–B) for the corresponding *E* isomer when L=CO, NH_3, and PH_3. A closer examination of Fig. 7 shows that the points for the four isomeric pairs are displaced one above and one below the trend line, with the *Z* isomer always above. For the *trans* isomers, the B–B coupling constants increase as the ligand strength decreases, with ^1J(B–B) for CO < PH_3 < SH_2 ~ NH_3 < OH_2 < ClH. Thus, these coupling constants also increase as the complex binding energies decrease, with a slight reversal of NH_3 and SH_2.

Figure 9 illustrates an inverse linear correlation between ^1J(B–H) and the computed MP2/6-31+G(d,p) electronic

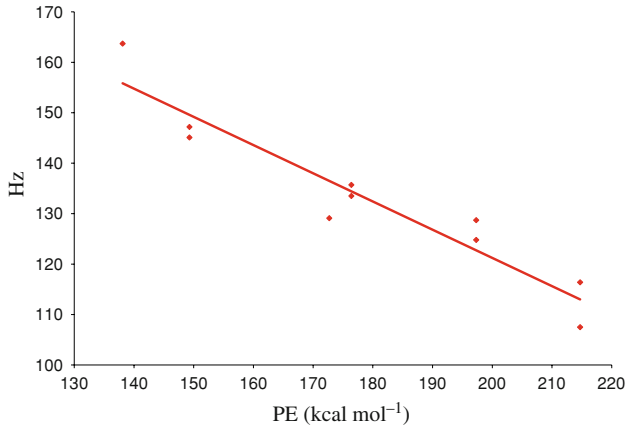

Fig. 9 ^1J(B1–H3) versus the protonation energy (PE) of the ligand L

protonation energy of the Lewis base L, with a correlation coefficient of 0.903. This indicates that ^1J(B–H) is also sensitive to the electron-donating ability of L. Once again, the grouping of the isomeric pairs is evident. Perhaps what is even more interesting is the observation that while ^1J(B–H) correlates with the protonation energy of L, there

is no correlation between the protonation energy and ^1J(B–B). Rather, as noted above, the B–B coupling constants appear to be inversely related to the ordering of L in the spectrochemical series. Thus, there is no correlation between changes in ^1J(B–B) and ^1J(B–H) in the series of complexes HLB=BLH.

4 Conclusions

An ab initio study has been carried out to investigate the structures, binding energies, bonding, and spin–spin coupling constants of complexes HLB=BLH, with L=CO, NH_3, OH_2, PH_3, SH_2 and ClH. The results of this study support the following statements.

1. Complex formation results in a lengthening of B–H and B–B bonds relative to singlet HBBH. For *trans* complexes in which the electron-donor atom of L is a second-period element, the shorter the B–X bond, the longer the B–B bond. A similar relationship is also found for *trans* isomers among complexes involving third-period elements. The B=B bond is always shorter in the *trans* isomer than in the *cis*.
2. All complexes HLB=BLH have singlet ground states, with the *trans* isomer more stable than the corresponding *cis* isomer. The order of stabilization energies correlates with the ordering of the ligands in the spectrochemical series of crystal field theory.
3. With the exception of H(OC)B=B(CO)H, the B–B bonds are essentially double bonds, with B–B bond orders that are not very sensitive to the nature of the ligands except for L=PH_3 and SH_2. It appears that a strong hyperconjugative interaction is primarily responsible for decreasing the B–B bond order in these two complexes. The complexes with CO show a different bonding pattern as CO acts as a strong σ-electron donor and π-electron acceptor.
4. One-bond B–B and B–H coupling constants, ^1J(B–B) and ^1J(B–H), are dominated by the Fermi-contact term, and are always positive. ^1J(B–B) and ^1J(B–H) are inversely related to the B–B and B–H distances, respectively. ^1J(B–B) for *trans* complexes also tends to correlate inversely with the ordering of ligands in the spectrochemical series and therefore with the binding energies of the complexes. ^1J(B–H) exhibits an inverse correlation with the protonation energy of the ligand.

Acknowledgments This work was supported by the DGI Project Nos. BQU-2003-00894, BQU2003-06553, and BQU-2003-01251 and the Project MADRISOLAR, ref S-0505/PPQ/0225 of the Comunidad Autónoma de Madrid. The continuing support of the Ohio Supercomputer Center is gratefully acknowledged.

References

1. Greenwood NN, Earnshaw A (1984) Chemistry of the elements. Pergamon Press, Oxford
2. Davidson MG, Wade K, Marder TB, Hughes AK (2000) Contemporary boron chemistry. Royal Soc Chem Cambridge
3. Marder TB, Lin Z (2008) Contemporary metal boron chemistry I. Borylenes, Boryls, Borane σ-complexes, and Borohydrides, Springer
4. Del Bene JE, Elguero J, Alkorta I, Yáñez M, Mó O (2006) J Phys Chem A 110:9959–9966
5. Mó O, Yáñez M, Martín-Pendás A, Del Bene JE, Alkorta I, Elguero J (2007) Phys Chem Chem Phys 9:3970–3977
6. Del Bene JE, Mó O, Yáñez M (2009) Croat Chem Acta (in press)
7. Segawa Y, Yamashita M, Nozaki K (2006) Science 134:113–115
8. Del Bene JE, Alkorta I, Elguero J, Yáñez M, Mó O (2007) J Phys Chem A 111:419–421
9. Zhou M, Tsumori N, Li Z, Fan K, Andrews L, Xu Q (2002) J Am Chem Soc 124:12936–12937
10. Wang W, Quillian B, Wei P, Wannere CS, Xie Y, King RB, Schaefer HFIII, Schleyer PVR, Robinson GH (2007) J Am Chem Soc 129:12412–12413
11. Scheschkewitz D (2008) Angew Chem Int Ed 47:1995–1997
12. Li SD, Zhai HJ, Wang LS (2008) J Am Chem Soc 130:2573–2579
13. Wang Y, Quillian B, Wei P, Xie Y, Wannere CS, King RB, Schaefer HF, Schleyer PVR, Robinson GH (2008) J Am Chem Soc 130:3298–3299
14. Rivard E, Power PP (2007) Inorg Chem 46:10047–10064
15. Power PP (1999) Chem Rev 99:3463–3504
16. Noth H, Knizek J, Ponikwar W (1999) Eur J Inorg Chem 11:1931–1937
17. Berndt A (1993) Angew Chem Int Ed 32:985–1009
18. Lee C, Yang W, Parr RG (1988) Phys Rev B 37:785–789
19. Becke AD (1993) J Chem Phys 98:5648–5652
20. Frisch MJ, Pople JA, Krishnan R, Binkley JS (1984) J Chem Phys 80:3265–3269
21. Frisch MJ, Trucks GW, Schlegel HB, Scuseria GE, Robb MA, Cheeseman JR, Montgomery Jr JA, Vreven T, Kudin KN, Burant JC, Millam JM, Iyengar SS, Tomasi J, Barone V, Mennucci B, Cossi M, Scalmani G, Rega N, Petersson GA, Nakatsuji H, Hada M, Ehara M, Toyota K, Fukuda R, Hasegawa J, Ishida M, Nakajima T, Honda Y, Kitao O, Nakai H, Klene M, Li X, Knox JE, Hratchian HP, Cross JB, Adao C, Jaramill, J, Gomperts R, Stratmann RE, Yazyev O, Austin AJ, Cammi R, Pomelli C, Ochterski JW, Ayala PY, Morokuma K, Voth GA, Salvador P, Dannenberg JJ, Zakrzewski VG, Dapprich S, Daniels AD, Strain MC, Farkas O, Malick DK, Rabuck AD, Raghavachari K, Foresman JB, Ortiz JV, Cui Q, Baboul AG, Clifford S, Cioslowski J, Stefanov BB, Liu G, Liashenko A, Piskorz P, Komaromi I, Martin RL, Fox DJ, Keith T, Al-Laham MA, Peng CY, Nanayakkara A, Challacombe M, Gill PMW, Johnson B, Chen W, Wong MW, Gonzalez C, Pople JA (2003) Gaussian 03. Gaussian, Inc., Pittsburgh
22. Pople JA, Binkley JS, Seeger R (1976) Int J Quantum Chem Quantum Chem Symp 10:1–19
23. Krishnan R, Pople JA (1978) Int J Quantum Chem 14:91–100
24. Bartlett RJ, Silver DM (1975) J Chem Phys 62:3258–3268
25. Bartlett RJ, Purvis DG (1978) Int J Quantum Chem 14:561–581
26. Hehre WJ, Ditchfield R, Pople JA (1972) J Chem Phys 56:2257–2261
27. Harihara PC, Pople JA (1973) Theor Chim Acta 238:213–222
28. Spitznagel GW, Clark T, Chandrasekhar J, Schleyer PVR (1982) J Comput Chem 3:363–371

29. Clark T, Chandrasekhar J, Spitznagel GW, Schleyer PVR (1983) J Comput Chem 4:294–301
30. Bader RFA (1990) In: Halpen J, Green MLH (eds) Atoms in molecules: a quantum theory; the international series of monographs of chemistry. Clarendon Press, Oxford
31. Bieger-König FW, Bader RFW, Tang TH (1982) J Comput Chem 3:317–328
32. Cramer D, Kraka E (1984) Croat Chem Acta 57:1259–1281
33. Becke AD, Edgecombe KE (1990) J Chem Phys 92:5397–5403
34. Silvi B, Savin A (1994) Nature 371:683–686
35. Noury S, Krokidis X, Fuster F, Silvi B (1999) ToPMoD Package, Universite Pierre et Marie Curie, 1997; Comp Chem 23:597–604
36. Reed AE, Curtiss LA, Weinhold F (1988) Chem Rev 88:899–926
37. Perera SA, Sekino H, Bartlett RJ (1994) J Chem Phys 101:2186–2191
38. Perera SA, Nooijen M, Bartlett RJ (1996) J Chem Phys 104:3290–3305
39. Perera SA, Bartlett RJ (1995) J Am Chem Soc 117:8476–8477
40. Perera SA, Bartlett RJ (1996) J Am Chem Soc 118:7849–7850
41. Schäfer A, Horn H, Ahlrichs R (1992) J Chem Phys 97:2571–2577
42. Dunning TH Jr (1989) J Chem Phys 90:1007–1023
43. Woon DE, Dunning TH Jr (1995) J Chem Phys 103:4572–4585
44. Kirpekar S, Jensen HJA, Oddershede J (1994) Chem Phys 188:171–181
45. Stanton JF, Gauss J, Perera SA, Watts JD, Yau AD, Nooijen M, Oliphant N, Szalay PG, Lauderdale WJ, Gwaltney SR, Beck S, Balková A, Bernholdt DE, Baeck KK, Rozyczko P, Sekino H, Huber C, Pittner J, Cencek W, Taylor D, Bartlett RJ, ACES II is a program product of the Quantum Theory Project, University of Florida. Integral packages included are VMOL (Almlöf J, Taylor PR); VPROPS (Taylor P); ABACUS (Helgaker H, Jensen HJA, Jørgensen P, Olsen J, Taylor PR); HONDO/GAMESS (Schmidt MW, Baldridge KK, Boatz JA, Elbert ST, Gordon MS, Jensen JJ, Koseki S, Matsunaga N, Nguyen KA, Su S, Windus TL, Dupuis M, Montgomery JA)
46. Dill JD, Schleyer PVR, Pople JA (1975) J Am Chem Soc 97:3402–3409
47. Treboux G, Barthelat JC (1993) J Am Chem Soc 115:4870–4878
48. Rozas I, Alkorta I, Elguero J (2000) J Am Chem Soc 122:11154–11161
49. Knop O, Boyd RJ, Choi SC (1988) J Am Chem Soc 110:7299–7301
50. Alkorta I, Barrios L, Rozas I, Elguero J (2000) Theochem 496:131–137
51. Mata I, Alkorta I, Espinosa E, Molins E, Elguero J (2007) In: Matta CF, Russell RJ (eds) The quantum theory of atoms in molecules: from solid state to DNA and drug design" pp 425–452, Wiley
52. Lynden-Bell RM, Harris RK (1969) Nuclear magnetic resonance spectroscopy. Appleton Century Crofts, New York